2023 62nd IEEE Conference on Decision and Control (CDC)
December 13-15, 2023. Marina Bay Sands, Singapore

Real-Time Optimisation-Based Robust Control: Heat Exchanger Comparative Analysis

Michaela Horváthová – Lenka Galčíková – Martin Klaučo – Juraj Oravec

***Abstract*— This paper investigates a possibility to improve the control performance of a laboratory-scale heat exchanger by introducing the convex-lifting-based robust controller into the closed-loop system. Robust model predictive control (MPC) design serves as the relevant reference control strategy. The improvements are expected in both, increased performance of the control trajectories and, simultaneously, reduced computational complexity. The performance is analyzed subject to the reference tracking implemented on the laboratory plate heat exchanger. This plant has a nonlinear and asymmetric behavior, affected by various uncertain parameters. The case study investigates the robust MPC, tunable convex-lifting-based robust control, and convex-lifting-based robust control with approximated control law. This paper also extends the convex-lifting-based robust control with approximated control law to provide the robust stability guarantees. The experimental case study evaluates and analyses various apprehensible criteria, e.g., energy consumption, carbon footprint, and computational demands.**

I. INTRODUCTION

Almost every industrial production, regardless of the type of particular industry, needs to facilitate some form of energy and heat transfer. To facilitate this heat transfer, heat exchanger devices are considered. The well-balanced control of these devices, minimizing the energy losses, maximizing the control performance, and eliminating the wasting of energy resources belong to the urgent tasks worth addressing. From the operation viewpoint, heat exchangers have challenging properties: the nonlinear and asymmetric behavior affected by various disturbances, e.g., piping transport delay, the impact of fouling, variable heat losses, etc. Therefore, the heat exchanger operation requires robust, tunable, and optimization-based controller design methods.

Nowadays, the most widely-used controllers for the operation of the heat exchangers are proportional-integral-derivative (PID) controllers [1], [2]. When it comes to heat exchangers, robustness is an important feature of the controller, due to all of the above-mentioned challenges.

In this work, we analyze the selected robust optimization-based controllers. The first is the robust model predictive controller (RMPC) as proposed in [7]. RMPC is often applied for heat exchangers due to its ability to guarantee safety and consider constraints, see [8], [9], [10]. Although the approach introduced in [7] is not a recent state-of-the-art method, it is a fundamental basis for many later introduced methods based on the evaluation of the linear matrix inequalities (LMI) see [11]. Moreover, its computational complexity is the lowest when compared to other LMI-based methods.

The convex-lifting-based methods are a less computationally demanding alternative to RMPC. As a consequence, this class of controller design methods is more suitable for industrial implementation. The convex-lifting-based robust control was initially proposed in [14]. In [15], the possibility to tune the convex-lifting-based method was introduced. This strategy was also applied for a heat exchanger in [16]. It was observed that sudden switching between multiple linear control laws as proposed in [15] causes input discontinuities, which decrease the control performance of the method. The convex-lifting-based control with approximated control law was introduced in [17], to overcome this drawback. The drawback of the approach proposed in [17] is that for the approximated control law there was no robust stability guarantee provided. This paper extends the approximated method proposed in [17] in order to provide the robust stability guarantees. To the authors' best knowledge, this paper offers the first laboratory implementation of the method proposed in [17] on a heat exchanger. To analyze the control performance and to evaluate the computational complexity, the methods proposed in [15] and [7], are also implemented considering the same plant.

We investigate the benefits of the robust control methods from the perspective of the closed-loop control performance and the computational complexity. Technically, the quality criteria investigated the control trajectories evaluating the settling time and maximal overshoot. The handling of control inputs was analyzed by the overall energy consumption and carbon footprint of a heat exchanger operation. The complexity of the robust control methods was analyzed by evaluating the computational time necessary to evaluate the optimal control action.

The authors gratefully acknowledge the contribution of the Slovak Research and Development Agency under the projects APVV-20-0261, APVV-21-0019, and the Scientific Grant Agency of the Slovak Republic under the grants 1/0297/22, 1/0545/20. Michaela Horváthová and Lenka Galčíková would like to thank for a financial contribution from the STU Grant scheme for Support of Teams of Young Researchers. This paper is funded by the European Union's Horizon Europe under grant no. 101079342 (Fostering Opportunities Towards Slovak Excellence in Advanced Control for Smart Industries)

Michaela Horváthová and Lenka Galčíková and Martin Klaučo and Juraj Oravec are with Institute of Information Engineering, Automation, and Mathematics; Faculty of Chemical and Food Technology; Slovak University of Technology in Bratislava, Radlinskeho 9, SK-812 37 Bratislava, Slovakia. michaela.horvathova@stuba.sk

II. Robust Control Methods

The main purpose of this paper is to analyze the control performance and computational complexity of various robust control methods implemented for a plate heat exchanger plant. We consider a discrete state-space model of the controlled plant affected by parametric and additive uncertainties

$$
\begin{aligned}
x(k+1) &= A(\Gamma)\, x(k) + B(\Gamma)\, u(k) + w(k), && \text{(1a)}\\
y(k) &= C\, x(k), && \text{(1b)}\\
x(0) &= x_0, && \text{(1c)}\\
[A(\Gamma), B(\Gamma)] &\in \operatorname{convhull}(A^{(\mathrm{v})}, B^{(\mathrm{v})}), && \text{(1d)}
\end{aligned}
$$

where k represents the discrete-time instant, $u(k) \in \mathbb{R}^{n_\mathrm{u}}$ are control inputs, $x(k) \in \mathbb{R}^{n_\mathrm{x}}$ stands for the system states and $y(k) \in \mathbb{R}^{n_\mathrm{y}}$ are the outputs of the system, and $w(k) \subset \mathbb{W} \in \mathbb{R}^{n_\mathrm{x}}$ represents a bounded additive disturbance. The matrices $A(\Gamma) \in \mathbb{R}^{n_\mathrm{x} \times n_\mathrm{x}}$, $B(\Gamma) \in \mathbb{R}^{n_\mathrm{x} \times n_\mathrm{u}}$, $C(\Gamma) \in \mathbb{R}^{n_\mathrm{y} \times n_\mathrm{x}}$, respectively are state, input, and output matrices of the system. The vector x_0 are the initial conditions of the system. The input and system matrices are defined using a convex hull to formulate the uncertain model of the system:

$$
A(\Gamma) = \sum_{v=1}^{n_\mathrm{v}} \Gamma_v A^{(v)}, \quad B(\Gamma) = \sum_{v=1}^{n_\mathrm{v}} \Gamma_v B^{(v)}, \tag{2}
$$

where $\Gamma_v \geq 0$, $\sum_{v=1}^{n_\mathrm{v}} \Gamma_v = 1$ and $v = 1, 2, \ldots, n_\mathrm{v}$ represents a v-th vertex of the polytopic uncertainty, where n_v is the quantity of the system vertices.

In order to ensure offset free control, the system states from (1) were augmented to include an integral action, creating the augmented vector of the system states $\widetilde{x}$.

$$
\widetilde{x}(k) = \begin{bmatrix} x(k) \\ \sum_{j=0}^{k} e(j) \end{bmatrix}, \tag{3}
$$

where $e(k) = r(k) - y(k)$ and $r(k) \in \mathbb{R}^{n_\mathrm{y}}$ denotes the reference. Considering the vector of augmented states in (3), the state, input and output matrices $\widetilde{A}, \widetilde{B}, \widetilde{C}$ are defined as follows:

$$
\widetilde{A} = \begin{bmatrix} A & 0 \\ -t_\mathrm{s} C & I \end{bmatrix}, \widetilde{B} = \begin{bmatrix} B \\ 0 \end{bmatrix}, \widetilde{C} = \begin{bmatrix} C & 0 \end{bmatrix}, \tag{4}
$$

where t_s is the sampling time of discrete-time system in (1). The aim of considered robust control methods is to compute the gain matrix $K \in \mathbb{R}^{n_\mathrm{u} \times n_\mathrm{u} + n_\mathrm{y}}$ at each sampling time:

$$
u(k) = [K_\mathrm{P}(k) \quad K_\mathrm{I}(k)]\, \widetilde{x}(k), \tag{5}
$$

where $K_\mathrm{P}(k)$ and $K_\mathrm{I}(k)$, respectively are the proportional and the integral parts of the control law.

A. Convex-lifting-based robust control

Another optimisation-based robust control method was introduced in [15]. The robust controller design is performed in 2 stages: the *offline stage* serves for the construction of the robust controller, and the *online stage* running during the real-time control provides the optimal control input.

The offline stage produces the convex lifting $\mathbb{X}_\mathrm{lift}$, n, multiple tunable robust positively invariant (RPI) sets denoted by $\mathbb{Z}_j$, $j = 1, \ldots, n$, see [19]. Each RPI set $\mathbb{Z}_j$ is a subset of RPI set $\mathbb{Z}_{j-1}$. For each RPI set, there is assigned a gain matrix K_j.

During the online stage the computation of optimal control inputs is ensured using either linear feedback control—assuming none of the physical constraints are active. Otherwise, using linear programming (LP)—if some physical constraint are active. The technical details are described in [20]. However, the approach proposed in [20] was not tunable and the achieved control performance was given in advance.

To overcome this obstacle, multiple tunable RPI sets $\mathbb{Z}_1 \ldots \mathbb{Z}_n$ are constructed based on the MPC-like weighting matrices (Q_j, R_j) tuned by the user, where every j-th pair of the weighting matrices is tuned to satisfy the following criteria:

$$
V_j(\widetilde{x}(0)) \leq -\sum_{k=0}^{\infty} \left(\|\widetilde{x}(k)\|_{Q_j}^2 + \|u(k)\|_{R_j}^2 \right), \tag{6}
$$

where V is the quadratic Lyapunov function

$$
V_j(\widetilde{x}) = \widetilde{x}^\top P_j \widetilde{x}, \quad P_j = P_j^\top \succ 0. \tag{7}
$$

The following SDPs were derived to optimize the control performance ensured by the parametrized control law [15]:

$$
\min_{\gamma_j, X_j, Y_j} \quad \gamma_j \tag{8a}
$$

$$
\text{s.t.:} \begin{bmatrix} X_j & \star & \star & \star \\ \widetilde{A}^{(v)} X_j + \widetilde{B}^{(v)} Y_j & X_j & \star & \star \\ Q_j^{1/2} X_j & 0 & \gamma_j I & \star \\ R_j^{1/2} Y_j & 0 & 0 & \gamma_j I \end{bmatrix} \succeq 0, \tag{8b}
$$

where the variable $\gamma_j > 0 \in \mathbb{R}$, $Y_j \in \mathbb{R}^{n_\mathrm{u} \times n_\mathrm{x}}$ represents the auxiliary matrix. X_j denotes the weighted inverted Lyapunov matrix $X_j = X_j^\top \succ 0 \in \mathbb{R}^{n_\mathrm{x} \times n_\mathrm{x}}$. During the offline stage, the SDP in (8) is solved and the associated j-th convex-lifting-based controller gain is computed as follows:

$$
u(k) = K_j\, \widetilde{x}(k) \tag{9}
$$

and the gain matrix is given by

$$
K_j = Y_j\, X_j^{-1}. \tag{10}
$$

In this paper, we consider an effective switching between 2 control laws K_1, K_2. The values of the gain matrices depend on the tuning parameters defined by the user, the MPC-like weighting matrices (Q_1, R_1), (Q_2, R_2) corresponding to each RPI set. It was shown in [15], that considering 2 RPI sets $\mathbb{Z}_1$ and $\mathbb{Z}_2$, represents a well-balanced trade-off between the closed-loop control performance on the plant side and the computational complexity on the controller side. By tuning of the weighting matrices (Q_j, R_j) associated to jth RPI set, we enforce $\mathbb{Z}_1$ to be *large-damped* RPI set and $\mathbb{Z}_2$ to be *small-aggressive* RPI set.

The *large-damped* RPI set $\mathbb{Z}_1$ is designed to have the maximal largest volume, which leads to minimization of the need to solve LP in the online stage. As a consequence, it leads to a decreased convergence (*damped*) rate of system states into the origin. The *small-aggressive* RPI set $\mathbb{Z}_2$ is designed to have an increased convergence rate of the system states to the origin. However, with increased convergence, the volume of the RPI set is decreased, i.e., $\mathbb{Z}_2 \subset \mathbb{Z}_1$. Technical details can be found in [15]. Obviously, considering multiple RPI sets and multiple linear control laws, sudden switching between associated controller gains occurs as the states shift from one RPI set to another. The sudden switching may lead to a decreased control performance.

B. Approximated convex-lifting-based robust control

The main objective of the approximation is to provide smoother switching between the control laws. Sudden switching arises when the states of the system shift from the outer *large-damped* set $\mathbb{Z}_1$ to the inner *small-aggressive* set $\mathbb{Z}_2$. This switching may have a negative impact on control performance when applied to certain types of processes. The approach was proposed in [17].

In this approach, a linear interpolation is considered, if the system states are present in the set difference of the *large-damped* RPI set and *small-aggressive* RPI set, i.e., $x \in \mathbb{Z}_1 \wedge x \notin \mathbb{Z}_2$. The approximation is based on the Euclidean distance of the states from the origin $d(k)$ during the real-time control. To perform the linear interpolation, minimal possible $d_{\min}$ and maximal possible distance $d_{\max}$ of the states from the origin, is computed.

The maximal admissible distance $d_{\max}$ is determined by the radius r_1 of the minimum-volume *outer approximation* of RPI set $\mathbb{Z}_1$, see Figure 1. Here, the value of the radius r_1 is determined by a ball with the smallest possible volume, so that the ball still includes RPI set $\mathbb{Z}_1$.

The value of the distance $d_{\min}$ from origin presented in *large-damped* RPI set $\mathbb{Z}_1$ is determined by the radius r_2 of the ball with maximal volume *inner approximation* that can be inscribed into RPI set $\mathbb{Z}_2$, see Figure 1. This class of approximation is referred to as the *Chebyshev ball* construction, e.g., see [21, p. 418].

The interpolated values are the proportional and integral parts of the gain matrix $K_{\text{approx}}(k) = [K_{\text{P,approx}}(k), K_{\text{I,approx}}(k)]$, both parts of the gain matrix are interpolated at each sample time k. The interpolated value replace the controller K_1 in the original control law in (9). Assuming that, the system states $x(k)$ belong to the *large-damped* set $\mathbb{Z}_2$, the gain matrix $K_{\text{approx}}(k)$ is interpolated based on the values of K_1, K_2 in (9) and the distance $d(k)$ as follows:

$$K_{\text{P,approx}}(k) = K_{\text{P},2} + (d(k) - r_2)\frac{K_{\text{P},1} - K_{\text{P},2}}{r_1 - r_2}, \quad \text{(11a)}$$

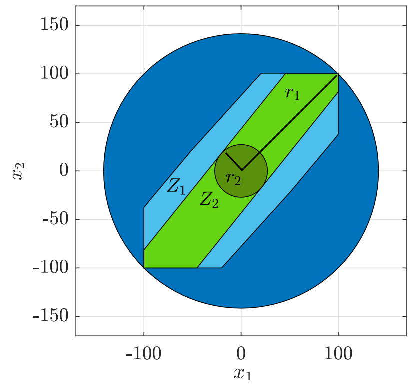

Fig. 1. Illustrative figure of the RPI sets: RPI set $\mathbb{Z}_1$ (bright blue), RPI set $\mathbb{Z}_2$ (bright green), the approximation of RPI set $\mathbb{Z}_1$ (dark blue), the approximation of RPI set $\mathbb{Z}_2$ (dark green) [17].

$$K_{\text{I,approx}}(k) = K_{\text{I},2} + (d(k) - r_2)\frac{K_{\text{I},1} - K_{\text{I},2}}{r_1 - r_2}, \quad \text{(11b)}$$

where $K_{\text{P},1}$, $K_{\text{P},2}$ and $K_{\text{I},1}$, $K_{\text{I},2}$ stand for the proportional and integral part of the controllers K_1 and K_2, respectively. The interpolated values $K_{\text{P,approx}}(k), K_{\text{I,approx}}(k)$ are computed at each sampling time based on the following rules:

$$u(k) = K_{\text{approx}}\,\widetilde{x}(k), \qquad \text{if} \quad \widetilde{x} \in \mathbb{Z}_1, \quad \text{(12a)}$$

$$u(k) = K_2\,\widetilde{x}(k), \qquad \text{if} \quad \widetilde{x} \in \mathbb{Z}_2. \quad \text{(12b)}$$

where the distance $d(k)$ varies in each sampling instant. As the approximation of the controller gain is performed using linear algebra, the associated control input is guaranteed to exist at each control step.

C. Stability Analysis of Approximated convex-lifting-based robust control

In [17], the closed-loop system stability of approximated convex-lifting-based robust control is guaranteed, only if the influence of parametric disturbance is considered in the uncertain system in (1). In that case, the closed-loop stability can be proven in the same manner as it is proven in [12]. The additive disturbance w in (1a) can be converted into the parametric uncertainty and vice versa, see [22]. In this paper, we propose a more straightforward way to directly enforce robust stability when the interpolated gain matrix is considered in the control law. Following the quadratic Lyapunov function defined in (7), suppose that $V(\widetilde{x})$ satisfies the following inequality:

$$V_j(\widetilde{x}(k+1)) - V_j(\widetilde{x}(k)) \leq 0. \quad \text{(13)}$$

Let us consider a pair of the gain matrices K_j and K_{j-1}, which satisfy the robust stability and the robust constraints in its RPI set. Then considering (13), it can be shown that the following condition holds:

$$X_j^{-1} - \Omega_{j-1}^{(v)\top} X_j^{-1} \Omega_{j-1}^{(v)} \succ 0, \quad \text{(14)}$$

where $\Omega_{j-1}^{(v)} = [A^{(v)} + B^{(v)} K_{j-1}]$, $j = 1 \dots n$, $v = 1 \dots n_{\mathrm{v}}$, see [23]. The satisfaction of (14) ensures robust stability for a convex combination of K_j and K_{j-1}. Note, the interpolation defined in (11) leads to a linear combination of two gain matrices. Then any value of gain matrix K_{approx} computed according to (14) assures robust stability, if the following condition holds:

$$X_1^{-1} - \Omega_{\mathrm{approx}}(k)^{(v)\top} X_1^{-1} \Omega_{\mathrm{approx}}^{(v)}(k) \succ 0, \quad (15)$$

where $\Omega_{\mathrm{approx}}^{(v)}(k) = (A^{(v)} + B^{(v)} K_{\mathrm{approx}}(k))$, $j = 1 \dots n$, $v = 1 \dots n_{\mathrm{v}}$. Therefore, the satisfaction of (15) is verified for $K_{\mathrm{approx}}(k)$ in each control step. If the condition (15) is not satisfied, then the last valid gain matrix $K_{\mathrm{approx}}(m)$ is implemented, where m denotes the control step when the valid control gain was evaluated. As the consequence, only the valid gain matrix K_{approx} is implemented in each control step.

III. Heat Exchanger Plant

The robust control methods presented in Section II were implemented on the laboratory liquid-liquid plate heat exchanger, manufactured by Armfield, see [24]. This device is illustrated.

The plate heat exchanger can be considered to cool or heat the liquid, in this case water. The cold liquid is stored in two tanks at the temperature $T_0 = 20^\circ$ C. The hot liquid is stored and heated to temperature $T_{\mathrm{hot}} = 70^\circ$ C inside a retention tank. The temperature of the hot liquid T_{hot} is sustained at constant temperature by an auxiliary PID controller. Both hot and cold liquids are pumped by two peristaltic pumps. The control output was the outlet temperature of the cold medium T. The control input represents the volumetric flow rate of the hot medium q. The main objective of the designed controllers was to heat or cool the cold liquid, ensuring reference tracking to the required value of output temperature T_{ref}.
As the heat exchanger plants has a nonlinear, asymmetric behaviour affected by uncertain parameters, the parameters of this device were identified as uncertain discrete-time state space model in (1). Further technical details regarding the model of the plant are in [25].

IV. Results and Discussion

In this case study, three robust control methods are analysed: (i) convex-lifting-based robust control (Section II-A), (ii) convex-lifting-based robust control with approximated control law (Section II-C), and (iii) robust MPC [7]. An extensive laboratory analysis is performed for each robust control method. The investigated performance criteria were focused on the evaluation of the closed-loop control performance of the reference tracking problem and the computational complexity.

A. Setup of laboratory experiments

The designed robust control methods were implemented using MATLAB/Simulink R2020b, installed on a PC with CPU i5 2.7 GHz and 8 GB RAM. YALMIP toolbox [26] was considered for the formulation and parsing of the optimization problems. The SDP was handled by the toolbox MUP [27], solver MOSEK v8 [28], and LPs by solver Gurobi [29]. The offline stage of the convex-lifting-based control is realized using the Multi-Parametric Toolbox [30]. Communication between the plant and the PC was secured using a Wifi-based eLab Manager toolbox [31]. Sampling time was set to $t_{\mathrm{s}} = 5\,s$.

The weighting matrices $\widetilde{Q}, \widetilde{R}$ were systematically tuned for RMPC design purposes to obtain:

$$\widetilde{Q} = \begin{bmatrix} 7 \times 10^{-1} & 0 \\ 0 & 5 \times 10^{-5} \end{bmatrix}, \quad \widetilde{R} = 30, \quad (16)$$

to ensure the required control performance of reference tracking problem. Two convex-lifting-based robust control design methods were implemented for the heat exchanger. The first method leads to switching between two control laws (Section II-A) and the other introduces the approximated control law (Section II-C). The robust controllers are designed by tuning the two pairs of weighting matrices:

$$Q_1 = \begin{bmatrix} 0.1 & 0 \\ 0 & 0.1 \end{bmatrix}, \quad R_1 = 1, \quad (17a)$$

$$Q_2 = \begin{bmatrix} 0.9 & 0 \\ 0 & 0.9 \end{bmatrix}, \quad R_2 = 1. \quad (17b)$$

These two pairs of weighting matrices for convex-lifting-based methods were systematically tuned to ensure required level of control performance.

B. Control performance analysis

The main objective of the designed robust control methods was to compute the optimal value of control input ensuring the offset-free reference tracking in the presence of uncertain parameters. All of the designed methods computed the optimal control action at each sampling time, however, the computational complexity differed with each method. Therefore, this paper investigates the control performance of these methods as well as their computational complexity.
The control performance of the implemented methods depends mainly on the tuning of the weighting matrices in (16) and (17). The weighting matrices were experimentally tuned until satisfactory control performance was achieved. The trajectories of the control output are depicted in Figure IV-B and the corresponding trajectories of the control input, i.e., the flow rate of the hot medium, are shown in Figure 2.
As can be observed in Figure IV-B, all of the robust control methods assured offset-free control, but all of the methods exerted a different control performance. The difference between RMPC and convex-lifting-based

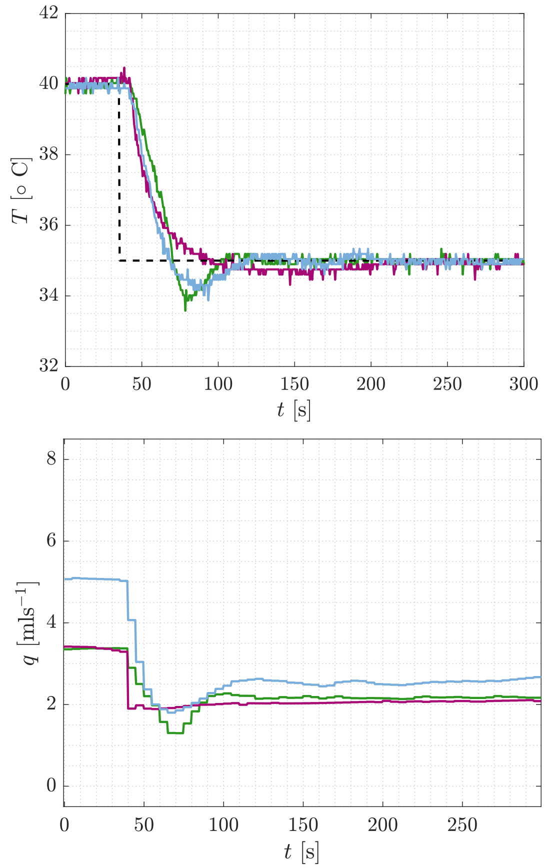

Fig. 2. The control trajectories generated using convex-lifting-based robust control (green), convex-lifting-based robust control with approximated control law (purple), and robust MPC (blue), and reference (dashed black).

methods is that RMPC was focused on the optimization of the worst-case system behavior. In this case, the uncertain vertex models were considered mainly to guarantee robust stability. On the contrary, the convex-lifting-based methods considered nominal system behavior in their design, see [15]. Nevertheless, the comparability of the methods is consistent, as the methods share the operating conditions and the same goal, which is to control the uncertain system and satisfy constraints on the control inputs and outputs.

From the perspective of the convex-lifting-based methods, in the offline stage, both used the same technique for construction of the convex lifting $\mathbb{X}_{\text{lift}}$ and RPI sets $\mathbb{Z}_1$, $\mathbb{Z}_2$.

The difference is in the online stage, when the method with approximated control law (Section II-C) computes the linear control law at each sampling time based on the interpolation (11), while the method without interpolation (Section II-A) applies the control laws computed in the offline stage.

The control perfromance was judged with respect to the evaluated criteria, which are summarized in Table I. Particularly, settling time t_{set}, maximal overshoot $\sigma_{\max}$, the energy consumption E and carbon footprint m_{CO_2} were analysed. The performance criteria in Table I were computed considering a time interval starting at time 35 s, when the reference step change occurred, and finishing at time 300 s.

Settling time t_{set} is computed as the time when the control output settles within 2 %-neighborhood of the setpoint value T_{ref}. Energy consumption E was evaluated as the overall energy exerted to heat the hot medium during the control time frame.

The energy consumption E served for evaluation of the carbon footprint m_{CO_2}. The detailed description of the computation of carbon footprint m_{CO_2} for the controlled plant can be found in [32].

TABLE I

Control performance criteria.

Method	t_{set}[s]	$\sigma_{\max}$[%]	E[kJ]	m_{CO_2}[g]
RMPC [7]	105	3.22	273	0.35
Section II-A	94	4.81	233	0.30
Section II-C	79	0.69	222	0.28

TABLE II

Computational complexity criteria.

Method	$V_{\text{RPI}}^{\text{I}}$ [$\times 10^3$]	$V_{\text{RPI}}^{\text{II}}$ [$\times 10^3$]	t_{RT} [ms]
RMPC [7]	31.4	1.9	160
Section II-A	7.8	6.8	1
Section II-C	7.8	6.8	50

The computational complexity of the methods was analyzed. Table II summarizes the computational complexity of the designed methods. Firstly, the average time to compute the optimal value of the control input during the real-time control t_{RT} was evaluated.

The convex-lifting-based robust control without the approximation reduced the computational by 99.4 % when compared to RMPC. This is caused by the fact that RMPC solves complex SDP optimization problems in each control step. In contrast to RMPC, convex-lifting-based robust control strategies solve either linear state feedback control law or LP.

In Table II, the values of V_{RPI}^{I} and V_{RPI}^{II} represent the volume of the RPI sets $\mathbb{Z}_1$, $\mathbb{Z}_2$ for convex-lifting-based methods. Both convex-lifting-based methods use the same RPI sets, therefore their volume is the same. In case of RMPC, parameters $V_{\text{RPI}}(1)$ and $V_{\text{RPI}}(2)$ represent the RPI set constructed for the current system measurement at the beginning and at the end of the closed-loop control, i.e., in time instants $t = 35$ and $t = 300$. As can be seen in Table II, RMPC is much more conservative, i.e., corresponding RPI set is larger, compared to RPI set generated for convex-lifting-based robust control method. On the other hand, the RMPC approach recomputes the RPI set at each time instant. As the consequence, its volume is shrinking and at the end of the control is smaller than the volume of RPI sets constructed for convex lifting.

The convex-lifting-based robust control with approximated control law evaluates $K_{\mathrm{P,approx}}(k)$ in (11) at each sampling time. It leads to the increased time t_{RT}. However, the increased computational complexity of the convex-lifting-based method with approximated control law is compensated by the significantly increased control performance of this method.

V. CONCLUSIONS

In this paper, we have applied multiple optimisation-based robust control methods for a laboratory-scaled plant. Moreover, this paper extended one of the optimisation-based methods towards providing robust stability guarantees. Using a laboratory case study, the heat exchanger, it has been demonstrated in (Figures IV-B, 2) that the implementation of the convex-lifting-based methods reduced almost all of the evaluated control performance criteria, except for the overshoot, see Tables I, II. The settling time was decreased by approximately 25 % and the maximal overshoot by 18 %. From the environmental viewpoint, the convex-lifting-based method outperformed RMPC also in the energy consumption E and the corresponding carbon footprint $m_{\mathrm{CO_2}}$ were reduced by 19 %. The convex-lifting-based method with approximated control law (Section II-C) also outperformed the method, where the sudden switching of control law occurs (Section II-A), in each investigated control performance criterion (Tables I, II).

References

[1] M. Trafczynski, M. Markowski, S. Alabrudzinski, and K. Urbaniec, "The influence of fouling on the dynamic behavior of PID-controlled heat exchangers," *Applied Thermal Engineering*, vol. 109, pp. 727–738, 2016.

[2] S. Diaz-Mendez, C. Patiño-Carachure, and J. Herrera-Castillo, "Reducing the energy consumption of an earth–air heat exchanger with a PID control system," *Energy Conversion and Management*, vol. 77, pp. 1–6, 2014.

[3] C. Mendil, M. Kidouche, and M. Doghmane, "Automatic control of a heat exchanger in a nuclear power station: The classical and the fuzzy methods," in *2019 International Conference on Advanced Electrical Engineering (ICAEE)*, pp. 1–6, 2019.

[4] A. Vasičkaninová, M. Bakošová, and A. Mészáros, "Fuzzy control design for energy efficient heat exchanger network," *Chemical Engineering Transactions*, vol. 88, pp. 529–534, Nov. 2021.

[5] M. Al-Dhaifallah, "Heat exchanger control using fuzzy fractional-order pid," in *2019 16th International Multi-Conference on Systems, Signals Devices (SSD)*, pp. 73–77, 2019.

[6] Z. Abdullah, M. H. Othman, and F. S. Taip, "Neural network based adaptive pid controller of nonlinear heat exchanger," in *2019 IEEE 9th International Conference on System Engineering and Technology (ICSET)*, pp. 453–458, 2019.

[7] M. V. Kothare, V. Balakrishnan, and M. Morari, "Robust constrained model predictive control using linear matrix inequalities," *Automatica*, vol. 32, pp. 1361–1379, 1996.

[8] L. Pekař and R. Prokop, "Algebraic robust control of a closed circuit heating-cooling system with a heat exchanger and internal loop delays," *Applied Thermal Engineering*, vol. 113, pp. 1464–1474, 2017.

[9] Y. Wang, S. You, W. Zheng, H. Zhang, X. Zheng, and Q. Miao, "State space model and robust control of plate heat exchanger for dynamic performance improvement," *Applied Thermal Engineering*, vol. 128, pp. 1588–1604, 2018.

[10] J. Oravec, M. Bakošová, A. Mészáros, and N. Míková, "Experimental investigation of alternative robust model predictive control of a heat exchanger," *Applied Thermal Engineering*, vol. 105, pp. 774–782, 2016.

[11] W.-J. Mao, "Robust stabilization of uncertain time-varying discrete systems and comments on "an improved approach for constrained robust model predictive control"," *Automatica*, vol. 39, no. 6, pp. 1109–1112, 2003.

[12] Z. Wan and M. V. Kothare, "Efficient robust constrained model predictive control with a time varying terminal constraint set," *Systems & Control Letters*, vol. 48, no. 5, pp. 375–383, 2003.

[13] H. Huang, D. Li, Z. Lin, and Y. Xi, "An improved robust model predictive control design in the presence of actuator saturation," *Automatica*, vol. 47, no. 4, pp. 861–864, 2011.

[14] N. A. Nguyen, S. Olaru, P. Rodríguez-Ayerbe, and M. Kvasnica, "Convex liftings-based robust control design," *Automatica*, vol. 77, pp. 206–213, 2017.

[15] J. Oravec, J. Holaza, M. Horváthová, N. A. Nguyen, M. Kvasnica, and M. Bakošová, "Convex-lifting-based robust control design using the tunable robust invariant sets," *European Journal of Control*, vol. 49, pp. 44–52, 2019.

[16] J. Oravec, M. Horváthová, and M. Bakošová, "Energy efficient convex-lifting-based robust control of a heat exchanger," *Energy*, p. 117566, 15 June 2020 2020.

[17] M. Horváthová, J. Oravec, and M. Bakošová, "Real-time convex-lifting-based robust control using approximated control law," in *59th IEEE Conference on Decision and Control*, vol. 59, (Jeju Island, Republic of Korea), pp. 2160–2165, IEEE, 2020.

[18] S. Boyd, L. E. Ghaoui, E. Feron, and V. Balakrishnan, *Linear Matrix Inequalities in System and Control Theory*. Philadelphia, USA: Society for Industrial and Applied Mathematics, 1994.

[19] F. Blanchini, "Set invariance in control," *Automatica*, vol. 35, pp. 1747–1767, 1999.

[20] N. Nguyen, M. Gulan, and S. P. Rodriguez-Ayerbe, "Convex lifting: Theory and control applications," *IEEE Transactions on Automatic Control*, vol. 63, pp. 1243–1258, 2018.

[21] S. Boyd and L. Vandenberghe, *Convex optimization*. New York, USA: Cambridge University Press, 2004.

[22] A. Bemporad and M. Morari, "Robust model predictive control: A survey," in *Robustness in Identification and Control*, pp. 207–226, Springer London, 1999.

[23] P. Bumroongsri and S. Kheawhom, "An interpolation-based robust mpc algorithm using polyhedral invariant sets," in *2013 European Control Conference (ECC)*, pp. 3161–3166, 2013.

[24] Armfiled, "Extracts from instruction manual PCT23," 2007.

[25] J. Oravec, M. Bakošová, D. Pakšiová, N. Mikušová, and K. Batárová, "Advanced robust MPC design of a heat exchanger: Modeling and experiments," in *27th European Symposium on Computer Aided Process Engineering*, (Barcelona, Spain), pp. 1585–1590, Elsevier, October 1 -5, 2017 2017.

[26] J. Löfberg, "Yalmip : A toolbox for modeling and optimization in MATLAB," in *In Proceedings of the CACSD Conference*, (Taipei, Taiwan), 2004.

[27] J. Oravec and M. Bakošová, "Software for efficient LMI-based robust mpc design," in *Proceedings of the 20th International Conference on Process Control*, (Štrbské Pleso, Slovakia), pp. 272–277, June 9-12, 2015 2015.

[28] A. MOSEK, "MOSEK," 2022.

[29] O. Gurobi, "Gurobi optimizer reference manual," 2022.

[30] M. Herceg, M. Kvasnica, C. Jones, and M. Morari, "Multi-Parametric Toolbox 3.0," in *Proc. of the European Control Conference*, (Zürich, Switzerland), pp. 502–510, July 17–19 2013. http://control.ee.ethz.ch/~mpt.

[31] M. Kalúz, Ľ. Čirka, R. Valo, and M. Fikar, "Lab of things: A network-based i/o services for laboratory experimentation," in *Preprints of the 20th IFAC World Congress, Toulouse, France*, vol. 20, pp. 14028–14033, 2017.

[32] M. Horváthová, J. Oravec, M. Bakošová, and A. Mészáros, "Carbon footprint analysis of a laboratory plate heat exchanger control," *Chemical Engineering Transactions*, vol. 88, pp. 847–852, 2021.